



Initial observations of the impacts of infauna on portable free fall penetrometer measurements in sandy parts of Mobile Bay

Nina Stark^{1,2} · Kelly M. Dorgan^{3,4} · Nicola C. Brill¹ · Madeline R. Frey³ · Chesna Cox^{3,4} · Joseph Calantoni⁵

Received: 27 February 2023 / Accepted: 1 January 2024 / Published online: 12 February 2024
© The Author(s) 2024

Abstract

The seabed surface provides habitat for abundant and diverse fauna, whose burrowing activities have been shown to modify geotechnical properties of surface sediments. Whether these impacts affect geotechnical properties on larger scales of traditional measurements has not been well studied. This study represents an initial attempt to assess whether infaunal activity affects seabed properties on a scale relevant for, and therefore, detectable in portable free fall penetrometer measurements. Specifically, we examine sediment strength profiles of the upper 10–70 cm of sandy (poorly graded sand and muddy sand) seabed sediments in Mobile Bay, Alabama, USA, hypothesizing that infauna create heterogeneity in sediment structure that would lead to variability in PFFP vertical profiles as well as among replicate measurements at a site. Sediments were composed predominantly of sands, with only 17% of the sites featuring sand contents < 97% and median grain sizes ranging from 0.0987 to 0.3457 mm. Sediment strength generally decreased with a decreasing sand content, but variability was not explained by sand content alone. PFFP impacts in sandier sites (> 97% sand) were limited to the surface few cm, but considerable vertical and spatial variability in muddy sands and lower strength at sites with abundant burrowing infauna suggest that infaunal activities may affect PFFP measurements in these sediments.

Keywords Ecosystem engineering · Infauna · Portable free fall penetrometer · Seabed surface properties

1 Introduction

Seabed sediments have gained increasing attention in geotechnical engineering associated with offshore oil and gas exploration and exploitation, offshore renewable energy development, naval applications such as unexploded ordnance (UXO) detection, identification, and

remediation, coastal engineering applications from the development of erosion and scour mitigation measures to navigation and transportation infrastructure, and more recently regarding the prediction of erodibility and sediment dynamics (Briaud et al. 2001; Corella et al. 2014; Dorvinen et al. 2018; Keller 1974; Lunne 2012; Meadows et al. 2012; Small et al. 2014; Stark and Kopf 2011; Watts et al. 2003; Westgate and DeJong 2005). Some of the listed problems and applications require a detailed characterization of the geotechnical properties of seabed sediments in the uppermost centimeters to a meter. This includes shallow bearing capacity problems related to moorings, subsea cables and pipelines, UXOs, or sensor and monitoring devices, as well as erosion and scour mitigation, to name just a few. However, these near-surface sediments provide habitat for a variety of organisms that interact with the seabed sediments in different ways, potentially changing the geotechnical characteristics of the seabed on varying temporal and spatial scales (Jones and Jago 1993; Meadows et al. 2012). Therefore, the understanding of

✉ Nina Stark
nina.stark@essie.ufl.edu

¹ Virginia Tech, Charles E. Via, Jr. Department of Civil and Environmental Engineering, Blacksburg, VA 24061, USA

² Present Address: University of Florida, Engineering School of Sustainable Infrastructure and Environment (ESSIE), Gainesville, FL 32611, USA

³ Dauphin Island Sea Lab, Dauphin Island, AL 36528, USA

⁴ School of Marine and Environmental Science, University of South Alabama, Mobile, AL 36688, USA

⁵ Naval Research Lab, Stennis Space Center, Hancock County, MS 39529, USA

interactions between benthic infauna and geotechnical seabed properties is crucial to assess the validity of geotechnical site characterization and assign appropriate variabilities and uncertainties when using geotechnical properties of seabed sediments in design, particularly for applications in the upper meter of the seabed surface. However, the costs and efforts associated with in situ geotechnical measurements of the seabed, the focus on deeper sediment characterization (with neglect of the uppermost tens of centimeters), and also the potentially high spatial and temporal variability of abundance and activity levels of infauna has so far limited the availability of data sets that relate geotechnical data of the seabed surface with infauna abundance and characterization. Most existing studies focus on impacts on the scales of centimeters in the context of habitats for infauna [e.g., (Clemon et al. 2022; Jones and Jago 1993; Meadows and Tait 1989)] rather than the impacts on larger-scale geotechnical measurements.

Infauna modify particle and bulk sediment properties like grain size distribution. For example, head-down deposit feeders that selectively ingest finer particles produce biogenic graded beds (Rhoads and Stanley 1965). Infauna also modify bed structure (i.e., stratification, porosity) and surface roughness (Rhoads and Cande 1971), as well as sediment strength parameters such as undrained shear strength (Rhoads and Boyer 1982). These effects are depth dependent on small (a few cm) scales; e.g., clams decrease shear strength in the top 2.5 cm but increase it at 2.5–7.5-cm depth (Rhoads and Boyer 1982). They vary between communities with different dominant species or functional groups, e.g., between burrowers and tube builders (Jacquot et al. 2018; Rhoads and Boyer 1982). The tube-building worm *Lanice conchilega* increases the stiffness of sediments (measured as shear wave velocity), whereas burrowers or burrow constructors decrease sediment rigidity (Jacquot et al. 2018; Rowden et al. 1998). Effects also, unsurprisingly, depend on the density of animals: Burrow construction also increases shear strength (measured using a Geonor fall-cone penetrometer), but only at medium to high densities of burrowers (Meadows and Tait 1989). Construction of burrows and tubes increases sediment permeability (Jones and Jago 1993; Meadows and Tait 1989), but active burrowers that disrupt relic burrows may decrease permeability. Tubes constructed from shell hash scatter high-frequency sound, increasing acoustic attenuation (Dorgan et al. 2020), whereas burrow creation and excavation of sediments by subsurface feeding and defecation on the surface reduces bulk density and therefore sound speed (Clemon et al. 2022). Barry et al. (2013) documented seasonal changes in yield strength, Young's modulus, and tensile fracture toughness

in the upper 20 cm on a tidal mudflat known for its abundant infauna.

Portable free fall penetrometers have increasingly been used to characterize seabed properties, particularly where seabed sediments in the upper meter of the seabed surface are investigated, or where time or access restrictions prohibit the use of standard cone penetration testing. PFFPs have a diameter of 4–11 cm, and their readings are affected by sediment properties within an area possibly 4 times as wide as the probe's diameter; being much larger than individual organisms or than the vane shear measurements used in laboratory experiments that have shown impacts of fauna on sediment strength (Meadows and Tait 1989; Rowden et al. 1998), there is some evidence that the impacts of infauna on geotechnical properties are substantial enough and extend to spatial scales large enough to alter sediment stability and therefore PFFP data. DeJong et al. (2014) assembled profiles of undrained shear strength obtained from penetrometer deployments with seabed sediment depth from five independent studies and locations. They documented an increase of undrained shear strength by 1–12 kPa (an approximate onefold to 12-fold increase) from bioturbation of marine worms in the upper 100 cm of the seabed surface. Stark and Wever (2009) showed variations in penetrometer deceleration records in the upper 15 cm of muddy sediments in Kiel Bay, Germany, from bioturbation and the presence of gas. Consolvo et al. (2020; 2022) studied effects of nearby oyster reefs on seabed surface sediment characteristics and observed a noticeable contribution through the intermixing of shells and shell fragments. It should be noted that while it has been hypothesized that benthic biogenic processes are reflected in portable free fall penetrometer measurements (Stark and Wever 2009), and thus, that infauna affect the geotechnical properties of the seabed sufficiently to be detected by a cone penetrometer with a diameter on the order of 4–11 cm (DeJong et al. 2014), the lack of detailed data allowing a direct comparison, particularly in sandy sediments and for different types of infauna, has limited those discussions to hypotheses and suggestions.

Infaunal species abundances and community structures are well established to exhibit patchy spatial structures on local scales of meters to 10 s or 100 s of meters (Herman et al. 2001; Meadows and Tait 1989). Patchiness can result from small-scale disturbances such as ray feeding pits that remove infauna and sediment and are subsequently filled through deposition of fine sediments and colonization by potentially different faunal communities (Levin 1984). This patchiness can coincide with variability in sediment properties, e.g., along a transect perpendicular to ripples in a muddy sand flat, different taxa were found in the ripple peaks that had high shear strength and lower organic content than in the troughs (Meadows et al. 2012). This

patchiness can be maintained by ecosystem engineering activities of fauna (Herman et al. 2001). Given this variability, multiple PFFP profiles may also vary within a site, e.g., due to patches of densely aggregated small animals or a region of impact around a larger animal versus relatively undisturbed sediments. PFFP data clearly distinguish sands from muds, with greater deceleration and shallower penetration depth in sands (Albatal and Stark 2017; Stark and Wever 2009; Stoll et al. 2007). The abundances and community composition of infauna as well as the mechanisms by which they affect sediment structure also vary between sands and muds, thus their impacts on PFFP in sands and muds are expected to differ (Meadows and Tait 1989). Note that infauna modify sediment structure more in muds than in sands.

The goal of this study was twofold: (1) Initially, assess whether infaunal activity affects seabed properties on a scale relevant for, and therefore, detectable in portable free fall penetrometer (PFFP) measurements collected in sandy seabed sediments of Mobile Bay, Alabama, USA. (2) Discuss PFFP measurements of the upper 10–70 cm of sandy seabed sediments in the context of infaunal communities in Mobile Bay, Alabama, USA. Specifically, we hypothesize that sites with greater fines content have both more infauna and more variability in PFFP profiles on small vertical scales consistent with heterogeneity created by burrowing activities. Additionally, we hypothesize that sites with more infauna will also have greater variability among PFFP profiles indicating heterogeneity on small horizontal scales consistent with patchy infaunal activities. We also initially explore potential relationships between the functional roles of the taxa present and the potential impact on PFFP to provide insight into how different functional groups affect sediment structure. Here, we use a direct comparison data set, including infaunal abundance, community structure, and size, as well as significant variations in the portable free fall penetrometer profiles, from different sandy areas in Mobile Bay to test these hypotheses. However, it should be noted that this study is based on an initial and opportunistic data collection effort to investigate the relationships between infauna and PFFP, and thus, the sediment characterization is limited to grain size distributions.

2 Regional context

Mobile Bay is located on the Alabama coast in the northern Gulf of Mexico (Fig. 1). Several rivers introduce freshwater to this river-dominated microtidal estuary, with the Mobile River and the Tensaw River being the largest tributaries. The bay has an area of more than 1000 km² and a mean depth of 3 m, making it susceptible to wave-seabed

interaction and wave-driven sediment transport. Sediment plumes composed of riverine sediments and muds resuspended by wind waves are discharged through the mouth of the bay, between the Fort Morgan peninsula and Dauphin Island (Dinnel et al. 1990). Bedford and Lee (1994) conducted field measurements offshore off Mobile Bay slightly north of core location 19 (Fig. 1) documenting sandy silt with median grain sizes fluctuating between 65 and 40 μm, eastward directed horizontal flow velocities of 7–15 cm/s at a height of 50 cm above the seabed, horizontal flow velocities in the onshore direction of up to 7 cm/s and in the offshore direction of up to 6 cm/s, and vertical velocities < 1 cm/s, suggesting dominant longshore currents. Significant wave heights at an average water depth of ~ 6 m reached 88 cm during the experiment in August 1989. Sediment concentrations reached 18 mg/liter at 50 cm above the seabed during these low-moderate flow conditions, and the presence of ripples suggested wave-driven sediment dynamics. Within Mobile Bay, wind waves within the bay are sufficient to drive sediment dynamics, and the navigation channel represents a major sediment sink for migrating sediments, and benthic organisms contribute to mixing of surface sediments (Parson et al. 2015). Nearshore sediments are sandy, but much of the shallow bay is muddy with low abundance and biomass of benthic organisms (Jacquot et al. 2018). Infaunal abundance and biomass are higher near the mouth and in sandy sediments with some mud (60–80% sand) (Bedford and Lee 1994; Jaber 2022). Byrnes et al. (2004) investigated areas offshore of Mobile Bay as potential sites for sand mining, confirming the dominant longshore current and gradient from silty sediments to the west, influenced by the Mobile Bay plume, to sandy sediments in the east. Infaunal community composition varied along this gradient as well, with plume-influenced muddier sediments dominated by polychaetes.

3 Methods

Co-located portable free fall penetrometer (PFFP) deployments and sediment grab samples for infauna and grain size characterization were conducted at 36 sites during a joint data collection campaign in June, 2021 (Fig. 1). Additional sedimentological characterization of sediment cores and acoustic surveying was performed by collaborators but is out of the scope of this article. Also, PFFP deployments were carried out in additional locations. However, this article focuses solely on the locations where geotechnical and infauna data were obtained. In the following section, the data analysis of the PFFP data and infauna data is described, respectively. The joint analysis is limited to a qualitative comparison and discussion.

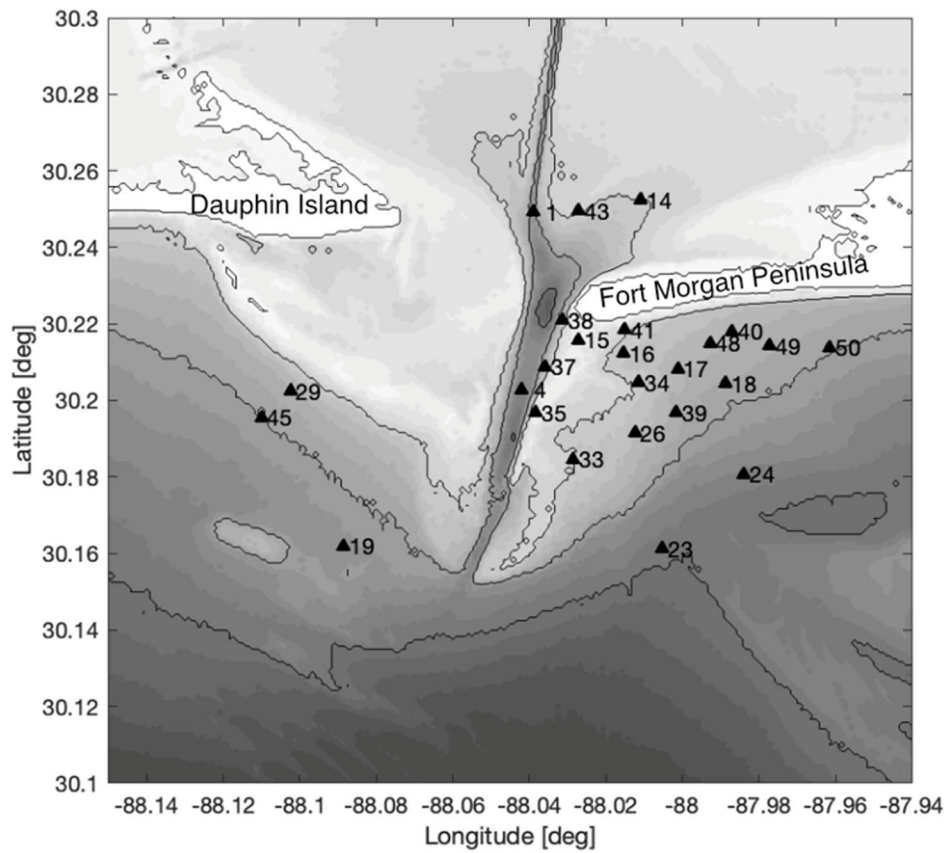


Fig. 1 (Top) Google earth image showing mobile bay and surrounding barrier islands. (Bottom) Map of the survey area at the mouth of the Bay with survey locations and numbers as triangles and depth contours shown as grayscale



Fig. 2 The portable free fall penetrometer *BlueDrop* during deployment

3.1 Portable free fall penetrometer (PFFP) measurements and analysis

The PFFP *BlueDrop* was used in this study (Fig. 2). The probe has a conical tip and a tapered body, allowing the assumption that the measured deceleration of the probe upon impact and penetration into the seabed is governed by sediment resistance against the conical tip. The probe has a weight of approximately 8 kg and a diameter of approximately 8 cm. Impact velocities after free fall in water are typically 4–6 m/s, and the resulting penetration depths are typically restricted to the upper 20 cm of the seabed surface in sands and reach > 100 cm in soft muddy sediments (Albatal and Stark 2017). Deceleration and ambient pressure behind the cone tip are measured at 2 kHz, enabling a vertical resolution of ~ 1 cm for the measured penetration profiles. Numerical studies of the same probe in sand suggest that the area of impact in sand featuring significant sediment displacement extends up to four times the probe diameter (i.e., as far as 28 cm from the penetrometer impact center) and that small sediment displacements extend up to seven times the probe diameter (i.e., 56 cm) from the penetrometer impact center (Zambrano-Cruzatty and Yerro 2020). This information is relevant when discussing scales between sediments affecting the penetrometer measurements and affected by infauna.

The probe measures its deceleration using five vertically oriented accelerometers with different measuring ranges and accuracies, tilt using 3-axes accelerometers, and ambient pressure using a pressure transducer behind the conical tip. Deceleration can be used to assess seabed soil properties directly (Stark and Wever 2009; Stoll et al. 2007), to derive parameters describing soil stiffness (Meadows and Tait 1989), or to estimate strength

parameters such as bearing capacity and undrained shear strength (Aubeny and Shi 2006; Dorvinen et al. 2018; Stark et al. 2012; Stark and Ziotopoulou 2017). Data quality control included checking the current calibration of the MEMS sensors, review of the entire time series in the context of the deployment procedure (handling, freefall, penetration, rest, and recovery), and review of measured inclination. Considering the expected shallow penetrations, it was assumed that inclination $< 10^\circ$ had negligible impacts (O’Loughlin et al. 2014); profiles with larger inclination at impact into the seabed were discarded from further analysis. In this study, the measured deceleration records will be directly compared to avoid bias from empirical factors or correlations. Relative density was estimated for sandy sediments following the approach by Albatal et al. (2020) through a customized calibration based on large calibration chamber tests. The firmness factor (FF) was determined following Mulutkutla et al. (2011), relating the maximum vertical deceleration (a_{\max}) measured over a penetration to the impact velocity (v_i) and penetration duration (t_i):

$$\text{FF} = \frac{a_{\max}}{g v_i t_i} \quad (1)$$

with g being the gravitational acceleration. Velocity and penetration depth are derived from the single and double integration of the deceleration-time curve. FF has been used for rapid sediment classification of seabed sediments using different free fall penetrometers (Albatal and Stark 2017; Mulutkutla et al. 2011).

3.2 Sediment and infauna characterization

A Van Veen sediment grab was used to collect sediments for granulometry and infauna. One grab sample from each site was sieved for infauna through a 500 μm mesh. Infauna were preserved in 95% ethanol stained with rose bengal, a tissue stain that facilitates picking animals from debris. Samples were sorted, and infauna identified to family level and measured in two dimensions (length and diameter) to estimate biovolume. Because our opportunistic sampling scheme did not provide enough replicates to quantitatively distinguish among sites (infauna samples are often variable), we focus on qualitative descriptions of key taxa or general patterns of abundance and community structure. Our aim here is to identify sites that have similar grain size distributions but differ in their infaunal community, particularly in the presence or absence of large taxa that we hypothesize based on their life history to have an impact on sediment structure. It should also be noted that in this exploratory study, no high-quality samples were available that would have allowed to perform direct or triaxial shear tests in the geotechnical laboratory to conduct

Table 1 Qualitative description of infaunal community data, grain size information, and expected impact on PFFP data at selected sites

Site	Lat; Long	Mean FF (m^{-1})	% Sand	d_{50} (mm)	Infauna summary	Expected impact	Penetrometer
1	30.2493354; – 88.039046	162.2	92.6	0.2486	Only 2 crabs	Low	
4	30.2029011; – 88.041934	360.75	99	0.2782	Small clams and epifauna	Low	
14	30.252372; – 88.010818	23.8	90.2	0.1669	Diverse infauna including burrowing worms, clams, shrimp, and brittle stars	Potential layering around patchy brittle star burrows around 6–10 cm deep	Some disruption at H47 at 10 cm, but distance between sites is 250 m
15	30.2158329; – 88.027146	360.5	100	0.3457	Small clams and epifaunal shrimp	Low, possible near-surface density reduction by clams	Hard sediments
18	30.2043882; – 87.988687	1103.6	100	0.1902	High abundance of infauna. Bivalves, snails, ice cream cone worms. Also burrowing shrimp and worms	Impact of hard-bodied or tube-building critters probably low due to high sand content, but there could be a bioturbated layer	Very hard
24	30.1807022; – 87.983977	39.8	92.5	0.1634	High abundance. Bivalves, epifaunal and burrowing shrimp, brittle stars, burrowing and tube-building small worms	Brittle star burrows 6–10 cm deep, surface likely bioturbated, potential increase in stiffness below 6–10-cm depth	Top 10 cm clearly disrupted
29	30.2024646; – 88.102502	76	72.7	0.1340	Small brittle stars, medium-sized clams, and some small worms	Possible burrow impacts and near-surface loosening, but brittle stars were small	Top 10 cm clearly disrupted
41	30.2185028; – 88.015069	1168	88.9	0.2129	Hermit crabs, snails, and epifaunal shrimp	Surface effects	Very hard; at some spots 1–2 cm loosening
43	30.2496333; – 88.027114	476.8	98.6	0.3594	Small clams and lancelets, lots of very small burrowing worms	Small surface effects	Very hard but with 2–3-cm looser top surface
45	30.1956306; – 88.110061	4.5	58.1	0.0987	Mantis shrimp, many clams, burrowing worms, and brittle stars	Probably fairly bioturbated with lots of burrows. Brittle star burrows to 6–10 cm, expect more resistance below bioturbated layer	Soft in spots and very disrupted

a more in-depth geotechnical seabed characterization beyond a grain size analysis.

4 Results

The PFFP results are expressed in terms of the measured deceleration versus penetration depth profiles, the firmness factor, and an estimate of relative density. PFFP results, sediment grain size distribution, and infauna were jointly reviewed at 36 sites. Possible impacts of infauna on surface sediment were hypothesized based on community data with no initial knowledge of the PFFP results.

Most locations featured > 90% sand content with median grain sizes (d_{50}) ranging from 0.1634 to 0.3457 mm (Table 1, Fig. 3). These sediments classify as

poorly graded sand to silty sand based on the Unified Soil Classification System (USCS; ASTM D 2487-06) or as fine to medium sand based on the Wentworth grain size classification. Two locations, MB45 (sand content = 58%, d_{50} = 0.0987 mm) and MB29 (sand content = 73%, d_{50} = 0.1340 mm), were considerably muddier classifying as clayey sand based on USCS or as very fine to fine sand after Wentworth (Fig. 3 right). Among the sandy sites, four were ~ 89–92% sand (termed “muddy sand” here; Fig. 3 center), and the rest were > 97% sand (“sandy”) (Fig. 3 left).

Mean firmness factors compared among all 36 sites were found to increase nonlinearly with sand content, but sites were predominantly sandy (sand content > 50% for all samples) (Fig. 4). Mean and range of the firmness factor of 4–6 PFFP replicate deployments at each site are shown

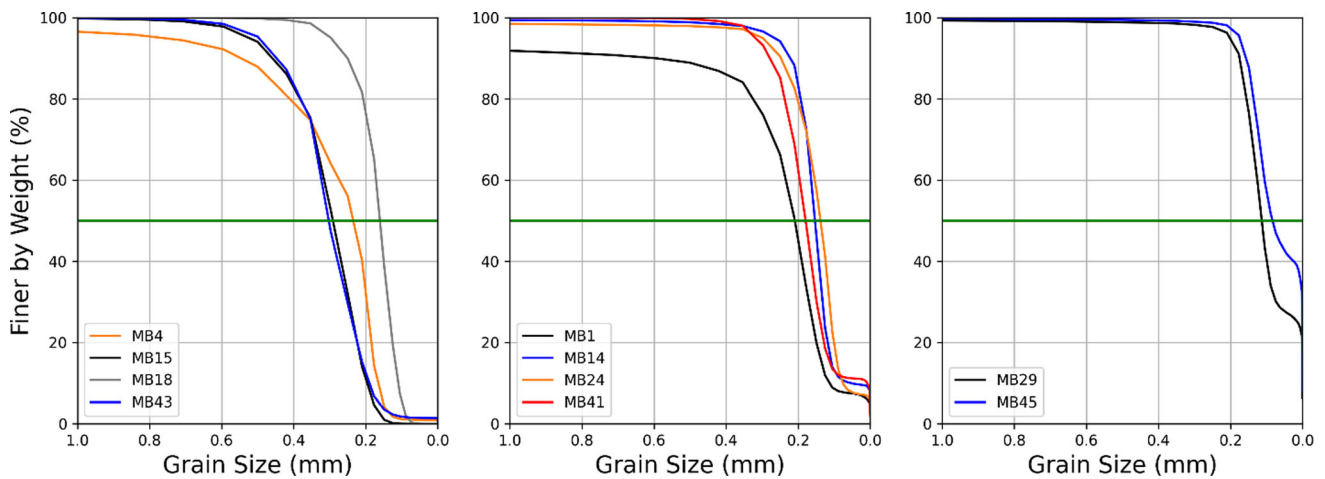


Fig. 3 Grain size distributions of selected sites from most sandy (> 97% sand content) (left) to most muddy (58–73% sand content) (right)

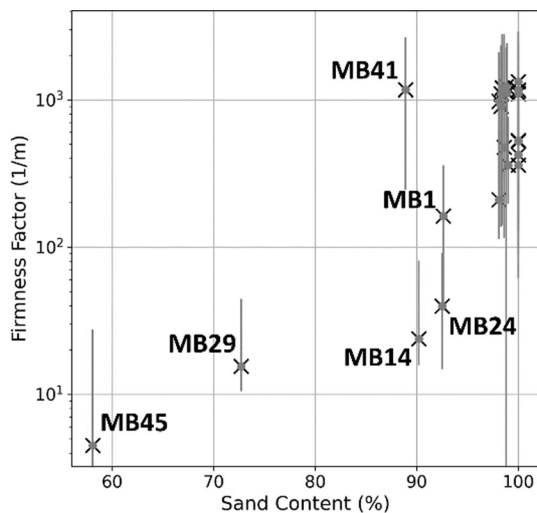


Fig. 4 Mean firmness factor (crosses) versus sand content for all sites. Range of replicate deployments is shown as gray errorbars. Low firmness factors (< 10) for high sand content (> 90%) are likely associated with inclined impacts (i.e., faulty deployments)

(Fig. 4 crosses, gray error bars). The smallest firmness factors $FF < 20 \text{ m}^{-1}$ were associated with locations MB45 and MB29 (sand content < 74%). There was considerable variability in firmness factor among the muddy sand sites, ranging from 24 m^{-1} at MB14 to very high ($FF > 1000 \text{ m}^{-1}$) for MB41. Based on Mulukutla et al.'s (Meadows and Tait 1989) firmness factor-based seabed classification scheme, MB45 falls within the range of coarse silt, MB14 as very coarse silt to very fine sand, and all other samples as sand. It should also be noted that those authors did not measure firmness factors $> 500 \text{ m}^{-1}$, but the PFFP used in their study was also of different geometry and weight. However, the same PFFP as in this study was used by Albatal and Stark (Albatal and Stark 2017), after

which MB45 classifies as clay and all other locations as sand, but they also did not measure firmness factors $> 100 \text{ m}^{-1}$. Thus, in this data set, most of the locations tested exhibited extremely hard seabed sediments even for sandy sediments ($FF > 500 \text{ m}^{-1}$). Interestingly, for sediments with sand contents $> 97\%$, the firmness factor varied substantially, with $FF = 210\text{--}1250 \text{ m}^{-1}$. However, FF of the sand sites appears to be bimodal, with one group clustered around $FF \approx 1000 \text{ m}^{-1}$ and another around $FF \approx 300 \text{ m}^{-1}$. More detailed review of median grain sizes (Table 1) or the detailed grain size distribution curves (Fig. 3) could also not explain the variability. Variability among the 4–6 replicate deployments was high for many sites, independent of sand content. In summary, the firmness factor analysis suggested very hard sandy sediments, exceeding values of two other studies (Albatal and Stark 2017; Meadows and Tait 1989). The variability of the firmness factor likely reflects spatial inhomogeneity. Sand content seemed to be related to firmness factor, consistent with previous studies (Albatal and Stark 2017; Meadows and Tait 1989), but MB14 and MB24 (sand contents 90–93%) were less firm than expected based on sand content and MB41 somewhat more firm. Those differences are aligned with small differences in grain size distributions (MB 14 and MB24 $d_{50} = 0.1634\text{--}0.1669 \text{ mm}$ and MB41 $d_{50} = 0.2129 \text{ mm}$; Table 1 and Fig. 3).

Both penetration depth and deceleration, and thus, also the firmness factor, depend strongly on sediment grain size (Fig. 4), so the sites were grouped by grain size to better compare sites with similar grain size but differing infaunal communities (Table 1). Among the sandy sites, we found epifaunal taxa such as mysid shrimp and hermit crabs, as well as small burrowing worms and amphipods that we expected to have minimal impact on sediment structure (Table 1). Some sites, e.g., MB43, had burrowing clams, whose exhalant siphons often expel water below the

sediment surface (Herman et al. 2001), as well as lancelets (~ 3.5 cm length). Lancelets, also called amphioxus, burrow with their posterior ends first into the sand and filter feed; when disturbed, they swim a short distance, then rapidly reburrow (Lambert 2005). Both clams and lancelets likely loosen the upper 2–3 cm of sand (Fig. 5). Among the muddy sand sites, MB14 and MB24 had rich infaunal communities with larger burrowing animals such as brittle stars and larger clams, whereas site MB41 had fewer infauna and MB1 had almost none. Site MB1 was in the channel, which is likely a more disturbed region due to scouring, dredging, and frequent hypoxia (Coogan et al. 2021). Both of the muddier sites (MB45 and MB29) had actively burrowing infauna. The muddiest site (MB45) had a mantis shrimp, which excavate large, deep burrows, and abundant clams, brittle stars and burrowing worms (Fig. 5). It is important to note that mantis shrimp have patchy distributions and our sampling was not sufficient to determine their distribution across the study area; we can only say that they were present at that site.

First, among sites with $> 97\%$ sand, PFFP deployments from three sites are shown representing the group with $FF \approx 300 \text{ m}^{-1}$, and MB18 is representative of deployments yielding $FF \approx 1000 \text{ m}^{-1}$. All of these deployments featured deceleration curves typical of those previously observed at sandy sites (Albatal and Stark 2017; Albatal et al. 2020; Stark and Wever 2009). The penetration depth is limited to < 8 cm (approximately equal to the cone length) for all deployments with this sand content. Loose

surface layers are limited to a sediment depth of 3–4 cm. The most notable difference among the sites with the very high sand contents is the maximum deceleration (ranging from about 40 g to > 100 g), which drives the two-group distribution of FF for the high sand content sites (Fig. 4). Considering the possible impact of the infaunal community on sites with sand contents $> 97\%$, no significant impacts were expected at sites MB4 (Figs. 6 and 7 left) and MB15, where small clams and epifaunal shrimp were found. Their near-surface activities are unlikely to affect sediment structure below the surface ~ 1 –2 cm, and thus, the relatively lower maximum deceleration and FF are unlikely to result from infaunal activity.

At MB18, where sand content was $> 98\%$, bivalves, snails, ice cream cone worms, and burrowing shrimp and worms were found, and we hypothesized there may be greater infaunal impact at that site. Maximum decelerations, however, exceeded 100 g, resulting in $FF > 1000 \text{ m}^{-1}$. This suggests hard sandy seabeds with little to no looser surface layer (Stark and Wever 2009; Stark and Kopf 2011). Following (Albatal et al. 2020), the penetrometer results suggest a relative density around 57% in the top 8 cm of the seabed surface. Loosening from infauna is not apparent in the PFFP data. The presence of hard-bodied infauna was noted for sites with $FF > 1000 \text{ m}^{-1}$ (including MB18) but was not unique to those sites. The PFFP data from site MB43 (Fig. 6 left blue line) suggested very hard sandy sediment similar to site MB18, and indeed, sand contents were $> 98\%$. However,

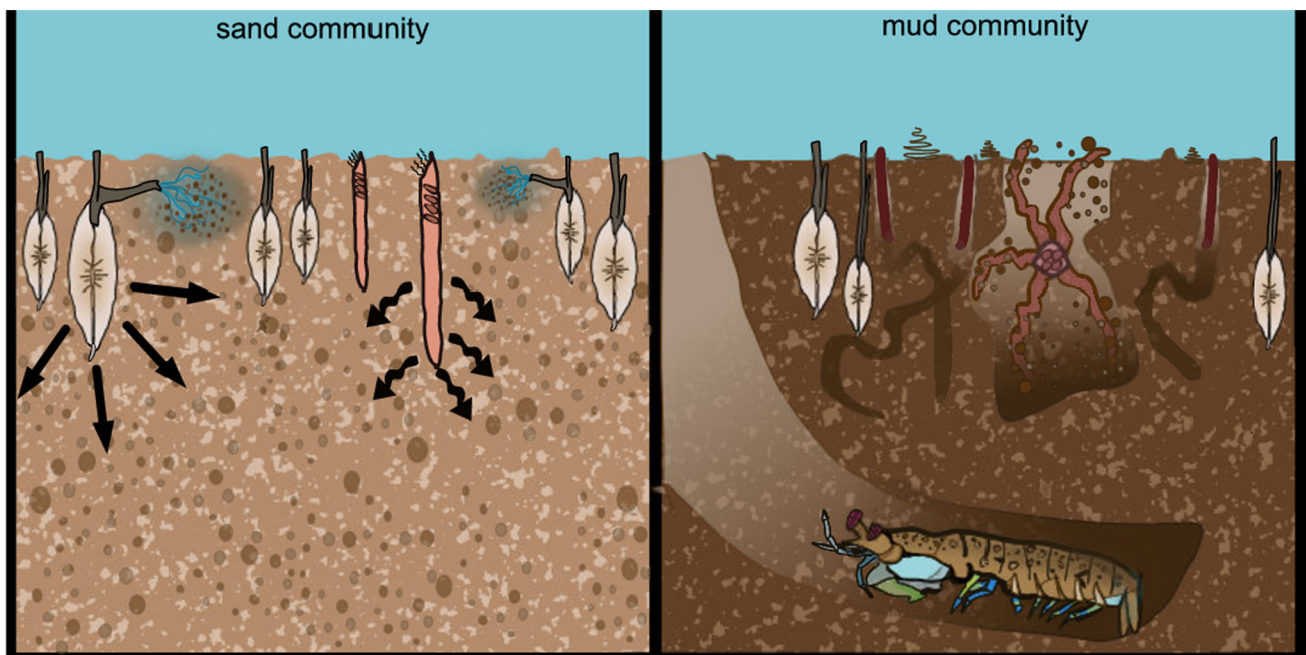


Fig. 5 Infauna found in **A** sandy and **B** muddy sediments that have behaviors and sizes most likely to impact PFFP data. **A** Clams and lancelets that may loosen surface sediments (e.g., site MB43). **B** Brittle stars, clams, burrowing shrimp, small burrowing and tube-building worms (e.g., site MB14)

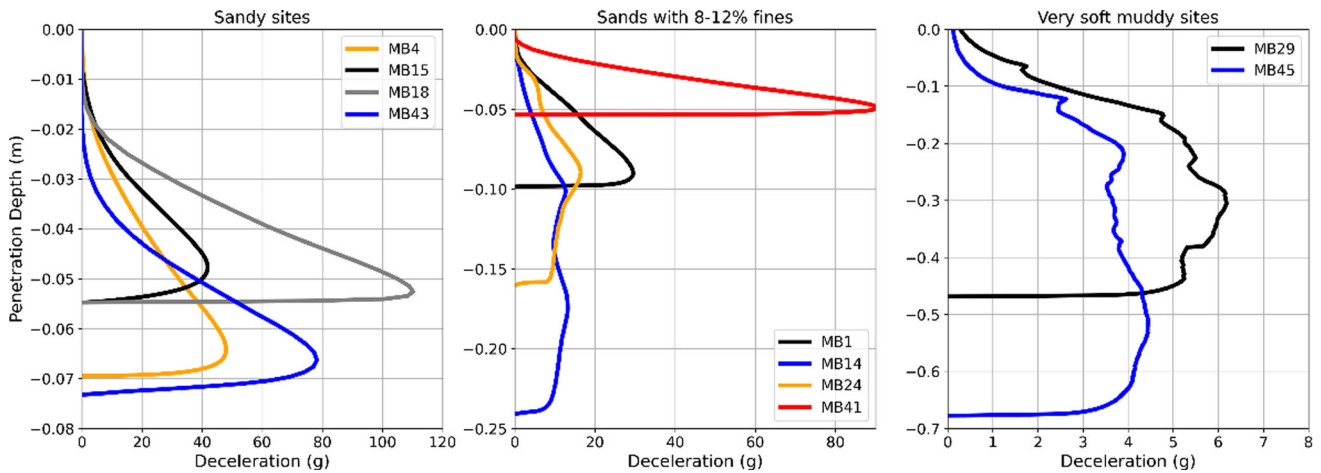


Fig. 6 Exemplary deceleration—depth profiles measured by the PFFP with sand content decreasing from the left to the right panel

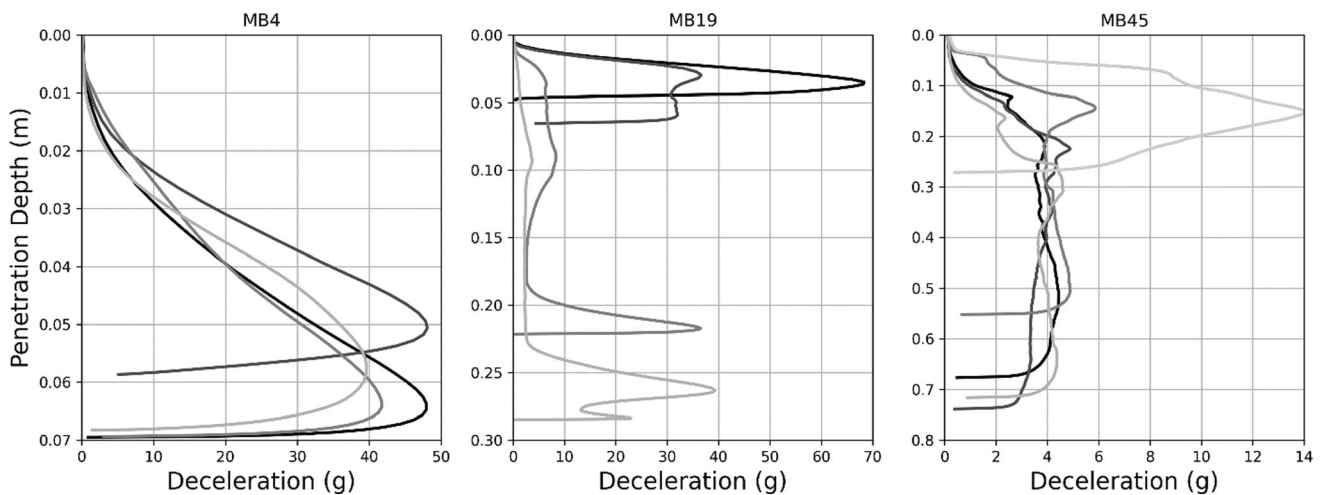


Fig. 7 Deceleration—depth profiles measured by the PFFP at MB4 (left), being one of sites with the highest consistency between the replicate PFFP deployments, MB19 (center), the site with the most outstanding variability between PFFP deployments at one site which was closely located to a dredge-spoil disposal site, and MB45 (right) where significant impacts from infauna were expected

the deceleration increases slightly deeper than at site MB18, and it may be argued that the top 2–3 cm appear looser. Small clams, lancelets, and worms were observed here that may have led to surface effects, but it should also be noted that this layer depth approaches the vertical resolution of the PFFP measurement, and similar observations have been made in areas of recent sediment deposition from active sediment dynamics. It follows that for sites with a sand content $> 97\%$ no significant weakening of sandy surface sediments was detectable in the PFFP data. Very hard seabeds ($FF > 1000 \text{ m}^{-1}$) featured the presence of hard-bodied infauna, but this presence was not exclusive to those sites. Therefore, no trends could be established without further information on abundance, combination of taxa with possibly contradicting effects, as well as patchiness in the context of scale of the PFFP and its duplicate deployments for sites with a sand content $> 97\%$. It should

also be noted that little impacts from infauna were expected at those sites.

Among the sites with 8–12% fines, sites MB14 and MB24 had rich infaunal communities, including burrowing brittle stars that we predicted would affect the sediment strength and increase variability in PFFP measurements in the upper 6–10 cm, whereas sites MB1 and MB41 had few infauna (Table 1). Interestingly, the PFFP data differed among these sites, consistent with expectations based on the infaunal community. Sites MB14 and MB24 (Fig. 6 center blue and orange lines), despite being in significantly different locations of the survey area (Fig. 1), exhibited similar PFFP responses of reduced maximum decelerations ($< 20 \text{ g}$) and a deeper penetration depth of 15–25 cm ($FF = 24 \text{ m}^{-1}$ and 40 m^{-1} , respectively), suggesting generally weaker sediments than at sites MB1 and MB41. Additionally, the deceleration–depth profiles from MB14

and MB24 show irregular deceleration, typically associated with vertical inhomogeneity of the sediments (Stark and Wever 2009). The maximum decelerations and penetration depths suggest loose sands at these sites (Albatal and Stark 2017). Considering an average maximum deceleration of ~ 14 g would suggest a relative density of sands of 11% (Albatal et al. 2020). Very high FF at site MB41 suggested hard sediments, which cannot be explained by the sand content (89%). Epifaunal hermit crabs, snails, and shrimp were observed here but few burrowing infauna.

The muddier sites, MB29 and MB45 also had rich infaunal communities, including clams, brittle stars and burrowing worms, hypothesized to lead to weaker, bioturbated sediments, particularly in the top 10 cm (Table 1). Mantis shrimp, which excavate burrows and are among the largest infauna found in this area, were found at MB45. PFFP data from these sites showed substantially lower maximum deceleration of < 8 g and deeper penetration depths of 47 and 70 cm, respectively (Figs. 6 and 7 right). Following (Albatal and Stark 2017; Mulukutla et al. 2011), this material behavior would be classified as clays or silts (MB45) to silty sands (MB29). However, sampling revealed 73% sand content for site MB29 and 58% sand content for MB45. While they would still in most classification frameworks be categorized as sand (clayey sand after USCS and very fine to fine sand after Wentworth), studies including (Jaber 2022; Jaber and Stark 2023) have suggested that cohesive behavior can dominate soil behavior and specifically the response to penetrators with fines contents of only 20–30%. However, the PFFP profiles measured at these sites not only suggest cohesive behavior, but soft sediments, particularly at site #45.

Infaunal abundances and community structures have been documented to vary substantially even on small spatial scales. This was also reflected in geotechnical data. Figure 7 compares replicate deployments at three sites: MB4 (high sand content, little expected infaunal impacts), MB19 (high sand content, likely affected by nearby dredge-spoil disposal site), and MB45 (clayey sand with expected high infaunal impacts on upper sediments). Replicate deployments were located within a radius of approximately 5 m, depending on the vessel stability and positioning system. All replicate deployments at MB4 are similar to each other (Fig. 7 left), meaning that all four deployments at this site suggested a similar seabed condition and strength. The replicate deployments at MB19 were highly variable with two suggesting a similarly hard seabed surface as seen at MB4 and two suggested 18–22 cm of softer material on top of a hard bottom. The latter observation suggests layering as it has been observed in areas of significant sediment dynamics as well as near fine-grained dredge-spoil disposal sites previously (Albatal and Stark 2017). The replicate deployments from MB45 are mostly

(4 out of 5) indicative of overall softer and finer grained sediments, but all replicate deployments featured irregularities (sharp peaks in the deceleration-depth profiles) which suggest disruption in a homogeneous soil matrix as it has been described for bioturbated sediments before (Stark and Wever 2009). At this location, indeed most infaunal impacts on sediments were expected based on the infauna characterization (Table 1). The disruptions were found down to sediment depths of 20–25 cm which is slightly deeper than anticipated based on the presence of infauna but can be explained with the penetrometer pushing sediment ahead of itself during penetration and having a larger zone of soil influence than its penetration depth and width (Zambrano-Cruzatty and Yerro 2020).

5 Discussion

The investigated sites in Mobile Bay were mostly sandy but varied in infaunal community and PFFP profiles. 83% of the sites tested featured a sand content $> 97\%$ and only one site had a sand content $< 60\%$. In most traditional soil classification frameworks, this seabed composition would be considered consistently sandy with most locations classifying as poorly graded sand and some as silty or clayey sand after the USCS. The interpretation of geotechnical parameters of sands from PFFP has initially received little attention due to the limited penetration depth of PFFP into sands. Stark et al. (2012) reinitiated this discussion by investigating the use of PFFP for sandy seabed investigations in the context of sediment dynamics. Later, White et al. (2018), Chow et al. (2018), and Albatal et al. (2020) proposed frameworks to estimate friction angles and relative density from free fall penetrometer measurements on sandy sediments. However, only the latter provided a validation of field testing with laboratory testing. Recently, Jaber and Stark (2023) tested a combined approach of these methods yielding an agreeable match between in situ estimates from PFFP with laboratory testing. Nevertheless, the interpretation of friction angles and relative density of sands from PFFP is still subject to research, and only (Jaber and Stark 2023) provided an initial discussion on how to treat mixed sediments. Furthermore, none of these studies included considerations of impacts from infauna or other soil structure disruptors. Therefore and in response to the lack of high-quality sediment samples for geotechnical laboratory testing, PFFP data analysis was limited to reviewing the measured deceleration, deriving the firmness factor as a proxy for sediment strength and type applied to a wider range of sediments, and estimates of relative density following (Albatal et al. 2020) to avoid impacts from uncertainty in data interpretation methods when discussing possible

effects of infauna on PFFP measurements in this exploratory study.

Although sediments were all sandy, maximum deceleration of the PFFP, firmness factor, and estimated relative density varied considerably among sites. Although there was a clear and expected positive relationship between firmness factor and sand content, there was considerable variability, especially among the muddy sand sites. In addition, there was a clear mismatch between PFFP interpretation and sediment composition for the muddiest sediments (e.g., PFFP suggested clay to silt for MB45 due to low resistance, but the sediment contained 58% sand). Some sandy sediments (e.g., MB41) had PFFP data indicating that they were significantly harder than similar sediment compositions measured in other studies. Considerable variability in firmness factor and deceleration was noted for very similar sediment compositions. Sediment dynamics and wave-seabed interactions can have hardening and softening effects on the seabed surface and create stratification (Bilici et al. 2019; Rowden et al. 1998). Active sediment dynamics have been documented in the area (Bedford and Lee 1994; Meadows et al. 2012), and sediment stratification indicative of effects of sediment dynamics was visible in sediment core samples retrieved by collaborators on the project, specifically distinct layers of sand over mud at sites within the Bay. Sand densification from wave action would be expected to be mostly limited to more nearshore environments, although sand deposition by storms has been documented within this study area. The dramatic variability observed within sites (Fig. 7) is unlikely to be related to sediment dynamics considering the observed variations in gradients (Fig. 6 center) and spikiness in deceleration profiles (Figs. 6 and 7 right) which suggest heterogeneity on smaller scales (replicate deployments within a radius of ~ 5 m) than would be expected from sediment dynamics (Rhoads and Boyer 1982; Rowden et al. 1998; Small et al. 2014). We also show results from MB19 which likely was affected by a nearby dredge-spoil disposal site in comparison to MB45 where expected highest influence from infaunal activity, and differences in the PFFP profiles are obvious with MB19 featuring clear layering while MB45 suggests rather disruptions of the soil matrix in the upper 20 cm of the seabed. Although we cannot discount sediment dynamics as a contributor to some of the variability observed, this small-scale variability and appearance of the disruption is likely better explained by infaunal activities contributing to sediment heterogeneity on scales that were reflected in the PFFP measurements. However, it should be noted that a spatial uncertainty of ~ 5 m is still larger than the scale of infauna patchiness in many locations, and thus, improved spatial accuracy in PFFP deployments and accurate knowledge of infauna locations would be required to

explore the effects of infaunal activity scale on PFFP deployments. This could be achieved through diver PFFP deployments in conjunction with high spatial resolution infaunal sampling.

In an effort to avoid bias in the comparative analysis, expected impacts of infauna on sediments were predicted prior to PFFP data analysis. For the sites with high sand contents ($> 97\%$), three possible effects were found. (i) Results (e.g., MB18) showed the presence of uncommonly hard surface sediments (firmness factor $> 1000 \text{ m}^{-1}$). DeJong et al. (2014) have suggested the presence of a hard seabed surface from bioturbation measured by penetrometers. Consolvo et al. (2020; 2022) highlighted strengthening effects from the presence of shell hash near oyster reefs. Hard surface sediments may be related to surficial bioturbation or possibly to the presence of shell fragments and hard-bodied infauna, but this cannot be confirmed from this study. Seabed densification from wave action could theoretically have a similar effect on the PFFP results; however, this seems unlikely based on comparison with previous measurements of sandy seabeds affected by wave action obtained by the same instrument (Albatal and Stark 2017). (ii) Results (e.g., MB15) also suggested possible softening of the upper 8 cm of sandy sediments by clams. If recent sediment deposition would be responsible for a loose surficial layer, it is commonly reflected in a clearly layered profile (Rowden et al. 1998) that is not visible at this site. (iii) MB43 featured a looser surface layer of ~ 2 cm. This may be a result of sediment dynamics. However, at the same site small clams and small burrowing worms were observed which would have had an impact only on very limited penetration depths (possibly 2 cm). Thus, the observed loose top layer at MB43 may have resulted from infauna or sediment dynamics.

Sites MB14, 19, and 24 featured quite irregular deceleration-depth profiles (i.e., changes in gradients of deceleration throughout the penetration). This is typically associated with vertical inhomogeneity which may represent stratification, hollows, pebbles, or shells. However, pebbles and shells typically lead to sharper gradients (Rhoads and Boyer 1982). Sites MB14 and 24 were the two muddy sand sites ($\sim 90\%$ sand) and higher abundances of larger-bodied, active burrowing infauna were found. For MB14 and 24, it is likely that lower strength and irregularity in the profiles (increases and decreases in strength with depth) reflect impacts of infauna. MB19 had a higher sand content in addition to the irregularity stratification. For MB19, it may be speculated that infauna affected this site as well, particularly since MB19 also featured significant variability among replicate deployments, which seems unusual while not impossible to result from sediment dynamics. However, since this site is located in the path of sediment plumes exiting the bay and near a dredge-

spoil disposal site, the significant variability and layering is likely governed by local sediment dynamics, human activity, or a combination of both.

For all three of these sites as well as MB 29 and MB45, the question arises if infauna expected predominantly in the uppermost 10 cm could affect the penetrometer readings down to about 20 cm of penetration depth. Zambrano-Cruzatty and Yerro (2020) show for the same PFFP and penetrations into sand that shear bands develop from the penetrometer tip to the surface down to the maximum penetration depths of about 20 cm in loose sands. It may be hypothesized that the irregularities observed reflect soil inhomogeneity from infauna in the upper 10 cm that still affect the penetrometer at penetration depths of 17 cm, or that the observations result from combined effects of sediment dynamics and infauna (e.g., recent sedimentation on infauna affected soil layers), but neither can be tested within this preliminary study. It is worth noting that the mean mixed layer depth of ~ 6–10 cm for bioturbation (Boudreau 1998; Teal et al. 2009) is based largely on chemical tracer profiles; longer preservation of the physical heterogeneities from bioturbation could result in deeper infaunal impacts.

Two sites (MB 29 and MB45, Fig. 5 right) had lower sand contents (< 80%) and, as expected, softer sediments. However, site MB45 seemed to have surprisingly soft sediments considering a sand content still > 50%, and both sites featured somewhat jagged deceleration-depth profiles. The latter often suggests small-scale disruptions like shell fragments or small pebbles that are too small and localized to change the overall trend but interrupt a smooth penetration, i.e., deceleration-depth profile (Stark and Wever 2009). Thus, it may be speculated that finer sediment contributions not only made the seabed softer, but that a larger abundance and activity of infauna exacerbated the sediment softening. A more detailed geotechnical analysis of these sites would be needed to fully test this hypothesis and understand the governing processes.

Spatial variability on the order of meters to sub-meter scales is well known for infauna but is rarely considered in geotechnical site investigation. The reason for the latter is that often geotechnical in situ testing of seabed sediments focus on larger scales, and surficial infauna effects are not of interest for the geotechnical site investigation. However, if geotechnical properties of the seabed surface are of interest to the investigation, ignoring this small-scale spatial variability from infauna may lead to significant mischaracterizations. Surficial sediments may be strengthened or weakened by infauna and may vary from lateral spatial inhomogeneity of infauna on sub-meter to meter-scales and much sharper vertical gradients. This may make replicate deployments not only important to test reliability of the measurements, but also to measure spatial inhomogeneity.

However, to-date there is no guidance on an acceptable and informative strategy.

The two issues of vertical and spatial inhomogeneity both of infaunal communities and their impacts on sediment geotechnical properties may be extended to a discussion of abundance and scale. Deviating impacts (strengthening and weakening) from infauna on PFFP-measured sediment strength may not only result from the actual benthic biogenic activity and process, but also the abundance of infauna and scales of organisms as well as their potentially patchy distributions. For example, some burrowing mechanisms may compact sediments on a small scale, e.g., along burrow walls, but the burrow itself represents a cavity, possibly leading to a weakening effect on the scale of the PFFP. It is important to note that our infaunal sampling was too limited to quantitatively compare among sites, making our comparison between infaunal community and PFFP results somewhat speculative. However, the variability both with depth and across replicate measurements at a site is consistent with predictions from the observations of infauna. Further research is needed to shed light on the observed variability and to make confident predictions on impacts of infauna on different scales of geotechnical measuring equipment or applications.

6 Conclusions

In this study, sediment composition, surficial seabed sediment strength, and infauna are related qualitatively (infauna) and to some degree quantitatively (portable free fall penetrometer deceleration-depth profiles, firmness factor, and estimated relative density as measures of sediment strength; sand content and grain size distributions) for seabed sediments in 36 locations in Mobile Bay, Alabama, USA. Sediments were composed predominantly of sands with only 17% of the sites featuring sand contents < 97%. Sediment strength generally decreased with a decreasing sand content, but considerable variability in sediment strength (for the firmness factor, almost an order of magnitude) was not explained by sand content alone. While we cannot exclude other soil mechanical impacts than sand content nor sediment dynamics (such as seabed bedform evolution, migration, and destruction, and generally local erosion and deposition processes particularly from storm events) as drivers for variability, infauna offered some reasonable explanations for variability, especially among the muddy sand sites ($\leq 90\%$ sand). Vertical and spatial variability, common and well acknowledged for infauna, were also observed in the penetrometer results, more so at sites with more infauna. To the best of the authors' knowledge, there is no guidance to-date on how to address

vertical and spatial inhomogeneity of sediment strength or proxies thereof in geotechnical site characterization on the scale of benthic biogenic processes. Increasing attention to sediment surface effects in subaquatic geotechnical engineering highlight the need for better understanding and integration of these processes in site characterization, especially for applications depending on textural and/or strength properties of seabed surface sediments (e.g., erosion, scour, and sediment dynamics, acoustics-seabed interaction, anchoring and mooring). Overall, this study highlights a still existing gap in knowledge regarding understanding the impacts of infauna on seabed sediment strength properties, its application in geotechnical problems and measuring techniques of different scale, and it also stresses a general lack of data to investigate those issues.

Acknowledgements This project was funded by ONR award #N00014-21-1-2214 to KMD, DoD SERDP award MR21-C1-1265 to NS and KMD, and NRL cooperative agreement #N00173-19-1-G018. We thank Cy Clemo for sampling infauna, Megan Ballard for providing the site map (Fig. 2), and Capt. Jonathan Wittmann and Diana Marchant for field assistance. We thank Sam Griffith and Ed Braithwaite for providing the detailed grain size analysis. We would also like to thank two anonymous reviewers and the associate editor Julian Tao for constructive comments that led to the improvement of this manuscript.

Funding Office of Naval Research, N00014-21-1-2214, Kelly M. Dorgan, Strategic Environmental Research and Development Program, MR21-C1-1265, Nina Stark, U.S. Naval Research Laboratory, N00173-19-1-G018, Nina Stark.

Declarations

Conflict of interest The authors have no competing interest related to the work. The datasets generated during and/or analyzed during the current study are available from the corresponding author on reasonable request. The infauna data are available through the Dauphin Island Sea Lab Data Center (<https://doi.org/10.57778/wsrc-jh08>).

Open Access This article is licensed under a Creative Commons Attribution 4.0 International License, which permits use, sharing, adaptation, distribution and reproduction in any medium or format, as long as you give appropriate credit to the original author(s) and the source, provide a link to the Creative Commons licence, and indicate if changes were made. The images or other third party material in this article are included in the article's Creative Commons licence, unless indicated otherwise in a credit line to the material. If material is not included in the article's Creative Commons licence and your intended use is not permitted by statutory regulation or exceeds the permitted use, you will need to obtain permission directly from the copyright holder. To view a copy of this licence, visit <http://creativecommons.org/licenses/by/4.0/>.

References

- Albatal A, Stark N (2017) Rapid sediment mapping and in situ geotechnical characterization in challenging aquatic areas. *Limnol Oceanogr Methods* 15(8):690–705. <https://doi.org/10.1002/lom3.10192>
- Albatal A, Stark N, Castellanos B (2020) Estimating in situ relative density and friction angle of nearshore sand from portable free-fall penetrometer tests. *Can Geotech J* 57(1):17–31. <https://doi.org/10.1139/cgj-2018-0267>
- Aubeny CP, Shi H (2006) Interpretation of impact penetration measurements in soft clays. *J Geotech Geoenviron Eng* 132(6):770–777. [https://doi.org/10.1061/\(ASCE\)1090-0241\(2006\)132:6\(770\)](https://doi.org/10.1061/(ASCE)1090-0241(2006)132:6(770))
- Barry MA, Johnson BD, Boudreau BP, Law BA, Page VS, Hill PS, Wheatcroft RA (2013) Sedimentary and geo-mechanical properties of Willapa Bay tidal flats. *Cont Shelf Res* 60:S198–S207. <https://doi.org/10.1016/j.csr.2012.05.007>
- Bedford KW, Lee J (1994) Near-bottom sediment response to combined wave-current conditions, Mobile Bay, Gulf of Mexico. *J Geophys Res Oceans* 99(C8):16161–16177. <https://doi.org/10.1029/94JC01226>
- Bilici C, Stark N, Friedrichs CT, Massey GM (2019) Coupled sedimentological and geotechnical data analysis of surficial sediment layer characteristics in a tidal estuary. *Geo-Mar Lett* 1(39):175–189. <https://doi.org/10.1007/s00367-019-00565-3>
- Boudreau BP (1998) Mean mixed depth of sediments: the wherefore and the why. *Limnol Oceanogr* 43(3):524–526. <https://doi.org/10.4319/lo.1998.43.3.0524>
- Briaud JL, Ting FCK, Chen HC, Cao Y, Han SW, Kwak KW (2001) Erosion function apparatus for scour rate predictions. *J Geotech Geoenviron Eng* 127(2):105–113. [https://doi.org/10.1061/\(ASCE\)1090-0241\(2001\)127:2\(105\)](https://doi.org/10.1061/(ASCE)1090-0241(2001)127:2(105))
- Byrnes MR, Hammer RM, Thibaut TD, Snyder DB (2004) Physical and biological effects of sand mining offshore Alabama, USA. *J Coastal Res* 20(1):6–24. <https://doi.org/10.2112/1551-5036>
- Chow SH, Bienen B, Randolph MF (2018) Rapid penetration of piezocones in sand. In: Proc., 4th Int. Symp. on cone penetration testing, pp 213–219. ISBN 978-1-138-58449-5
- Clemon WC, Giles KD, Dorgan KM (2022) Biological influences on coastal muddy sediment structure following resuspension. *Limnol Oceanogr*. <https://doi.org/10.1002/lno.12213>
- Consolvo S, Stark N, Castro-Bolinaga C, Massey G, Hall S, Campbell M, Thomas M (2020) Subaqueous sediment characterization near oyster colonies by means of side-scan sonar imaging and portable free-fall penetrometer. In: Geo-congress 2020: geotechnical earthquake engineering and special topics. <https://doi.org/10.1061/9780784482810.074>
- Consolvo ST, Stark N, Castellanos B, Castro-Bolinaga CF, Hall S, Massey G (2022) Effects of shell hash on friction angles of surficial seafloor sediments near oysters. *J Waterw Port Coast Ocean Eng* 148(5):04022015. [https://doi.org/10.1061/\(ASCE\)WW.1943-5460.0000716](https://doi.org/10.1061/(ASCE)WW.1943-5460.0000716)
- Coogan J, Dzwonkowski B, Lehrter J et al (2021) Observations of dissolved oxygen variability and physical drivers in a shallow highly stratified estuary. *Estuar Coast Shelf Sci* 259:107482. <https://doi.org/10.1016/j.ecss.2021.107482>
- Corella JP, Arantegui A, Loizeau JL, DelSontro T, Le Dantec N, Stark N, Girardclos S (2014) Sediment dynamics in the subaquatic channel of the Rhone delta (Lake Geneva, France/Switzerland). *Aquat Sci* 76(1):73–87. <https://doi.org/10.1007/s00027-013-0309-4>
- DeJong JT, Soga K, Kavazanjian E, Burns S, Van Paassen LA, Al Qabany A, Weaver T (2014) Biogeochemical processes and geotechnical applications: progress, opportunities and challenges. In: Bio-and chemo-mechanical processes in geotechnical engineering: géotechnique symposium in print 2013. pp 143–157. <https://doi.org/10.1680/bcmpe.60531.014>

- Dinnel SP, Schroeder WW, Wiseman WJ (1990) Estuarine-shelf exchange using landsat images of discharge plumes. *J Coast Res* 6:789–799
- Dorgan KM, Ballentine W, Lockridge G et al (2020) Impacts of simulated infaunal activities on acoustic wave propagation in marine sediments. *J Acoust Soc Am* 147:812–823. <https://doi.org/10.1121/10.0000558>
- Dorvinen J, Stark N, Hatcher B, Hatcher M, Leys V, Kopf A (2018) In situ assessment of sediment erosion and consolidation state using a free-fall penetrometer: Sydney Harbour, Nova Scotia. *J Waterw Port Coast Ocean Eng* 144(2):04017041. [https://doi.org/10.1061/\(ASCE\)WW.1943-5460.0000423](https://doi.org/10.1061/(ASCE)WW.1943-5460.0000423)
- Gadeken K, Dorgan K (2023) Sediment macrofaunal response to the diel oxygen cycle. *Mar Ecol Prog Ser* 703:67–80. <https://doi.org/10.3354/meps14217>
- Herman P, Middelburg JJ, Heip C (2001) Benthic community structure and sediment processes on an intertidal flat: results from the ECOFLAT project. *Cont Shelf Res* 21:2055–2071. [https://doi.org/10.1016/S0278-4343\(01\)00042-5](https://doi.org/10.1016/S0278-4343(01)00042-5)
- Jaber R (2022) Investigation of the relationships between geotechnical sediment properties and sediment dynamics using geotechnical and geophysical field measurements. PhD dissertation submitted to Virginia Tech. <https://vtechworks.lib.vt.edu/handle/10919/111284>
- Jaber R, Stark N (2023) Geotechnical properties from portable free fall penetrometer in coastal environments. *ASCE's J Geotech Geoenviron Eng* 149(12):04023120–04023121. <https://doi.org/10.1061/JGGEFK.GTENG-11013>
- Jacquot MP, Dorgan KM, Mortazavi B et al (2018) Macrobenthic community structure and influence on denitrification capacity in soft sediments (Mobile Bay, Alabama, USA). *Mar Ecol Prog Ser* 605:17–35. <https://doi.org/10.3354/meps12759>
- Jones SE, Jago CF (1993) In situ assessment of modification of sediment properties by burrowing invertebrates. *Mar Biol* 115:133–142. <https://doi.org/10.1007/bf00349395>
- Keller GH (1974) Marine geotechnical properties: interrelationships and relationships to depth of burial. *Deep-Sea Sediments*. Springer, Boston, MA, pp 77–100
- Lambert G (2005) Ecology and natural history of the protochordates. *Can J Zool* 83:34–50. <https://doi.org/10.1139/z04-156>
- Levin LA (1984) Life history and dispersal patterns in a dense infaunal polychaete assemblage: community structure and response to disturbance. *Ecology* 65:1185–1200. <https://doi.org/10.2307/1938326>
- Lunne T (2012) The Fourth James K. Mitchell Lecture: the CPT in offshore soil investigations—a historic perspective. *Geomech Geoeng* 7(2):75–101. <https://doi.org/10.1080/17486025.2011.640712>
- Meadows PS, Tait J (1989) Modification of sediment permeability and shear strength by two burrowing invertebrates. *Mar Biol* 101:75–82. <https://doi.org/10.1007/bf00393480>
- Meadows PS, Meadows A, Murray JMH (2012) Biological modifiers of marine benthic seascapes: their role as ecosystem engineers. *Geomorphology* 157–158:31–48. <https://doi.org/10.1016/j.geomorph.2011.07.007>
- Mulukutla GK, Huff LC, Melton JS, Baldwin KC, Mayer LA (2011) Sediment identification using free fall penetrometer acceleration-time histories. *Mar Geophys Res* 32(3):397–411. <https://doi.org/10.1007/s11001-011-9116-2>
- O'Loughlin CD, Gaudin C, Morton JP, White DJ (2014) MEMS accelerometers for measuring dynamic penetration events in geotechnical centrifuge tests. *Int J Phys Modell Geotech* 14(2):31–39. <https://doi.org/10.1680/ijpmg.13.00020>
- Parson L, Lovelace N, Godsey E, Reine K, Gailani J (2015) Regional sediment management (RSM) strategy for Mobile Bay, Alabama. Engineer research and development center Vicksburg MS coastal and hydraulics lab. <https://apps.dtic.mil/sti/citations/ADA614456>
- Rhoads DC, Stanley DJ (1965) Biogenic graded bedding. *J Sediment Res* 35:956–963. <https://doi.org/10.1306/74d713bb-2b21-11d7-8648000102c1865d>
- Rhoads DC, Cande S (1971) Sediment profile camera for in situ study of organism-sediment relations. *Limnol Oceanogr* 16:110–114. <https://doi.org/10.4319/lo.1971.16.1.0110>
- Rhoads DC, Boyer LF (1982) The effects of marine benthos on physical properties of sediments. Springer, Boston, MA, pp 3–52
- Rowden AA, Jago CF, Jones SE (1998) Influence of benthic macrofauna on the geotechnical and geophysical properties of surficial sediment, North Sea. *Cont Shelf Res* 18:1347–1363. [https://doi.org/10.1016/s0278-4343\(98\)00047-8](https://doi.org/10.1016/s0278-4343(98)00047-8)
- Small AA, Cook GK, Brown MJ (2014) The geotechnical challenges of tidal turbine projects. In: International conference on offshore mechanics and arctic engineering 45530: V09AT09A055. American Society of Mechanical Engineers. <https://doi.org/10.1115/OMAE2014-23892>
- Stark N, Wever TF (2009) Unraveling subtle details of expendable bottom penetrometer (XBP) deceleration profiles. *Geo-Mar Lett* 29(1):39–45. <https://doi.org/10.1007/s00367-008-0119-1>
- Stark N, Kopf A (2011) Detection and quantification of sediment remobilization processes using a dynamic penetrometer. In: OCEANS'11 MTS/IEEE KONA. pp 1–9. <https://doi.org/10.23919/OCEANS.2011.6106914>
- Stark N, Coco G, Bryan KR, Kopf A (2012) In-situ geotechnical characterization of mixed-grain-size bedforms using a dynamic penetrometer. *J Sediment Res* 82(7):540–544. <https://doi.org/10.2119/jsr.2012.45>
- Stark N, Wilkens R, Ernstsen VB, Lambers-Huesmann M, Stegmann S, Kopf A (2012) Geotechnical properties of sandy seafloors and the consequences for dynamic penetrometer interpretations: quartz sand versus carbonate sand. *Geotech Geol Eng* 30:1–14. <https://doi.org/10.1007/s10706-011-9444-7>
- Stark N, Ziotopoulou K (2017) Undrained shear strength of offshore sediments from portable free fall penetrometers: theory, field observations and numerical simulations. In: Offshore site investigation geotechnics 8th international conference proceeding. Society for Underwater Technology, pp 391–399. <https://doi.org/10.3723/OSIG17.391>
- Stoll RD, Sun YF, Bitte I (2007) Seafloor properties from penetrometer tests. *IEEE J Ocean Eng* 32(1):57–63. <https://doi.org/10.1109/JOE.2007.890943>
- Teal LR, Parker R, Fones G, Solana M (2009) Simultaneous determination of in situ vertical transitions of color, pore-water metals, and visualization of infaunal activity in marine sediments. *Limnol Oceanogr* 54(5):1801–1810. <https://doi.org/10.4319/lo.2009.54.5.1801>
- Watts CW, Tolhurst TJ, Black KS, Whitmore AP (2003) In situ measurements of erosion shear stress and geotechnical shear strength of the intertidal sediments of the experimental managed realignment scheme at Tollesbury, Essex, UK. *Estuar Coast Shelf Sci* 58(3):611–620. [https://doi.org/10.1016/S0272-7714\(03\)00139-2](https://doi.org/10.1016/S0272-7714(03)00139-2)
- Westgate ZJ, DeJong JT (2005) Geotechnical considerations for offshore wind turbines. Report for MTC OTC Project. https://www.researchgate.net/profile/Jason-Dejong/publication/252536016_Geotechnical_Considerations_for_Offshore_Wind_Turbines/links/555b4eb108ae91e75e76453a/Geotechnical-Con

[siderations-for-Offshore-Wind-Turbines.pdf](#)

White DJ, O’Loughlin CD, Stark N, Chow SH (2018) Free fall penetrometer tests in sand: determining the equivalent static resistance. In: Cone penetration testing 2018. pp 695–701. ISBN 978-1-138-58449-5

Zambrano-Cruzatty L, Yerro A (2020) Numerical simulation of a free fall penetrometer deployment using the material point method.

Soils Found 60(3):668–682. <https://doi.org/10.1016/j.sandf.2020.04.002>

Publisher’s Note Springer Nature remains neutral with regard to jurisdictional claims in published maps and institutional affiliations.